Supporting Information for

A Phase-transition-assisted Method for the Rational Synthesis of Nitrogen-doped Hierarchically Porous Carbon Materials for Oxygen Reduction Reaction

Wei Li, Wei Ding,* Jinxia Jiang, Qian He, Sicheng Tao, Wanglan Wang, Jing Li, Zidong Wei*

The State Key Laboratory of Power Transmission Equipment & System Security and New Technology, College of Chemistry and Chemical Engineering, Chongqing University, Chongqing, 400044, China.

E-mail: dingwei128@cqu.edu.cn (W, Ding)；zdwei@cqu.edu.cn (Z, Wei).

Synthesis of materials

Typically, 1 g iron citrate was mixed with 2 g ammonium chloride by grounding them in an agate ball mill for about 2 h. After that the pyrolysis of the obtained mixture was performed at 900 °C for 2 h under argon atmosphere with flow rate of 70 mL min^{-1} at the heating rate of 5 °C min^{-1}. The iron species in the resulted black solid (CNFe before acid etching) were washed off in a 0.5 M H_2SO_4 solution at 80 °C for 12 h. Finally, the products (CNFe) were collected by filtration, washed with abundant distilled water and dried at 60 °C for several hours. For comparison, CNNa and CNNaFe were synthesized by a similar route except using sodium citrate and the mixture of 0.5 g sodium citrate, 0.5 g iron citrate and 2 g ammonium chloride, as precursors instead of iron citrate. Besides, CFe and CNa were synthesized by direct pyrolysis of the single precursor iron citrate and sodium citrate, respectively at 900 °C.

Characterization

Field emission scanning electron microscopy (FE-SEM) spectroscopy images were obtained by Hitachi S-4800 (S-4800, FEI Ltd., Japan). X-ray photoelectron spectra (XPS) were acquired using a Kratos XSAM800 spectrometer equipped with a monochromatic Al X-ray source (Al KR, 1.4866 keV). The X-ray Diffraction (XRD) experiments were performed on an XRD-6000 (Japan) equipped with a Cu Kα (λ =0.15418 nm) radiation source. The scanning range of the 2θ angle was from 10° to 80° at a speed of 2° min^{-1}. Raman spectrum was recorded by a LabRamHR evolution Raman spectrometer equipped with an Nb-Yag laser excitation source operated at 532 nm.

Electrochemical ORR measurements

All electrochemical data was obtained by a conventional one-compartment three-electrode cell at room temperature. The standard cell was used with a glassy carbon (GC electrode, 3 mm in diameter, PINE: AFE3T050GC), an Ag/AgCl (saturated KCl) and a platinum foil as working electrode, reference electrode and counter electrode, respectively. In this paper, all potentials are relative to that of the reversible hydrogen electrode (RHE). We prepared the working electrodes by applying catalyst ink onto glassy carbon (GC) disk electrodes. Briefly, the electrocatalyst was completely dispersed in ethanol by 15 min ultrasonic to make sure the formation of a uniform catalyst ink. Then, 3 μL of the suspension was transferred onto the GC disk and the solvent was evaporated at room temperature. After drying, the surface of the catalyst layer was covered with one drop of 0.05 wt% Nafion solution to form a thin protective film. Before the electrochemical tests, the electrodes were dried overnight at room temperature. All the electrodes were firstly subjected to 30 potential cyclings between 0 and 1.2 V at a sweep rate of 50 mV s^{-1} prior to ORR activity testing, in order to remove possible surface contamination.

The Koutecky-Levich plots were performed by linearly fitting the reciprocal rotating speed versus reciprocal current density collected at various potentials from -0.1 V to -0.6 V. The electron transfer number was calculated from the following equation:

$$1/j_D = 1/j_k + 1/B\omega^{1/2}$$

$$B = 0.62nFC_{O2}D_{O2}^{2/3}v^{-1/6}$$

where n is electron transfer number per oxygen molecule involved in the ORR, C_{O2} is the bulk concentration of oxygen (1.2×10^{-6} mol cm^{-3}), D_{O2} is the diffusion coefficient of oxygen in the sulfuric acid solution (1.9×10^{-5} cm^2 s^{-1}) and ν is the kinematic viscosity of the sulfuric acid (0.01 cm^2 s^{-1}).

Electrochemical supercapacitor performance

Supercapacitor tests were carried out in a three-electrode electrochemical cell with 6 M KOH as aqueous electrolyte. A platinum foil was applied as a counter electrode with an Ag/AgCl electrode as a reference electrode. The preparation of working electrode was same with that used in the ORR tests. The electrochemical performance was determined by the galvanostatic charge-discharge tests at room temperature.
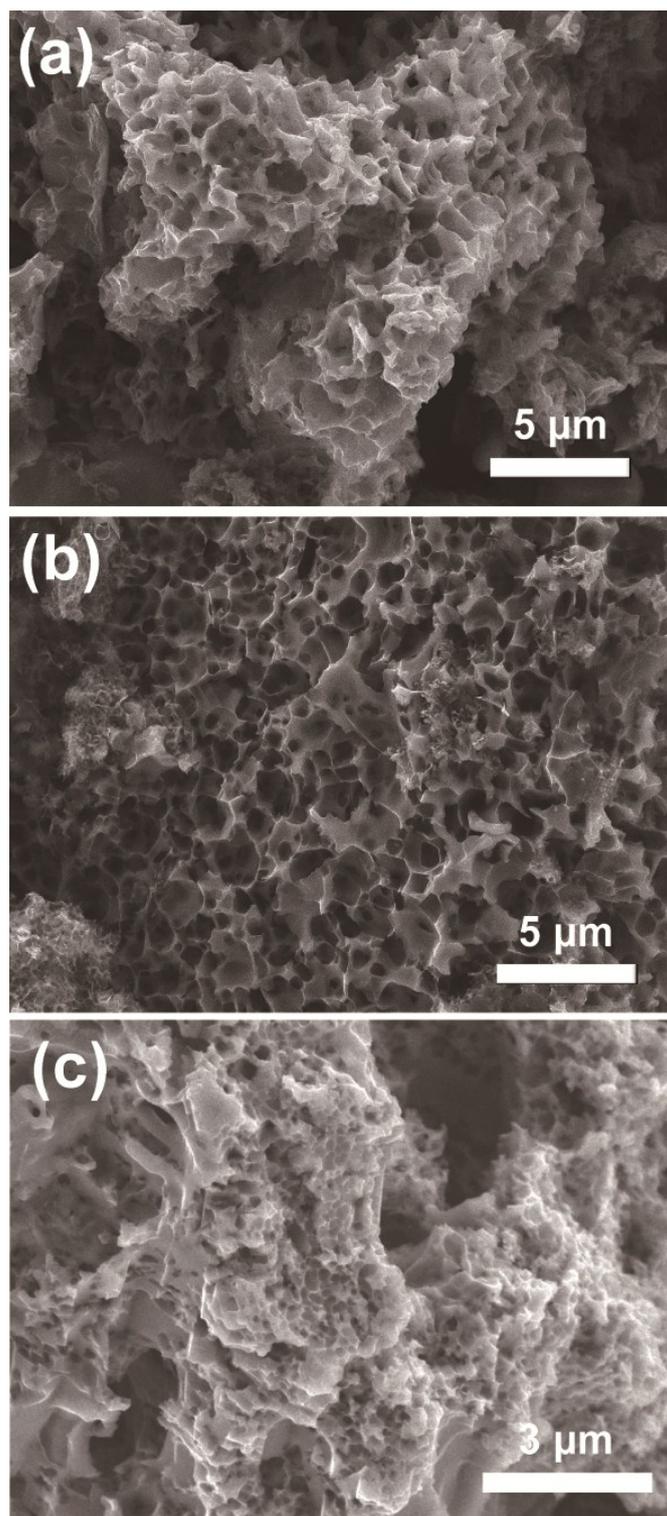
Fig. S1. SEM images of (a) CNNa, (b) CNNaFe, (c) CNFe.
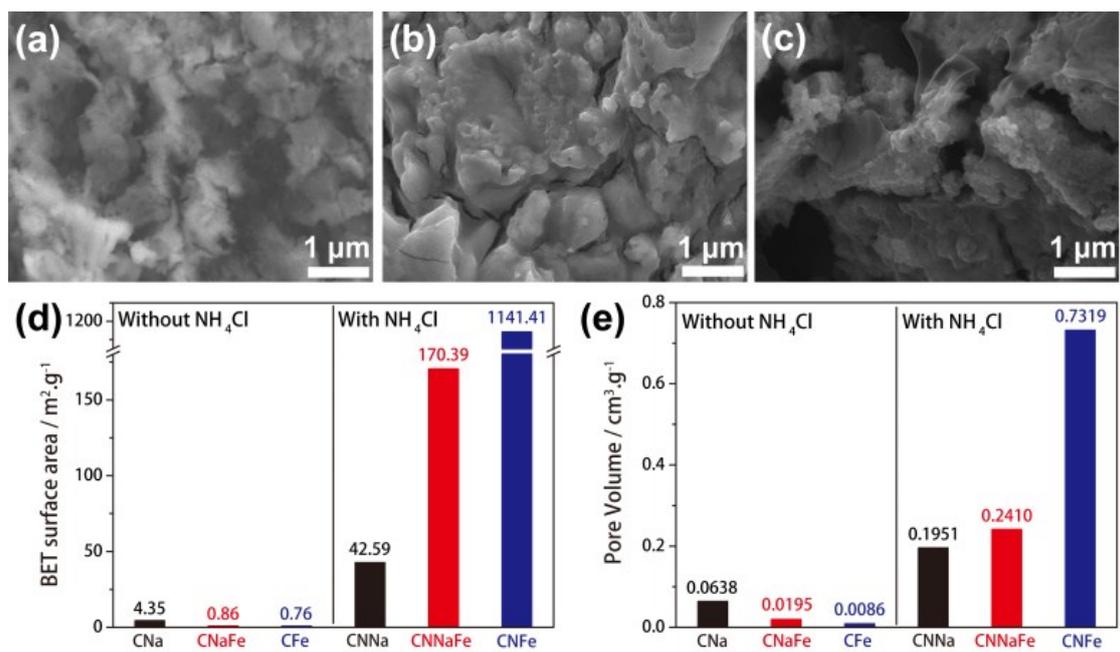
Fig. S2. SEM images of (a) CNa, (b) CNaFe, (c) CFe. (d) BET surface area and (e) Pore volume of HPCMs.
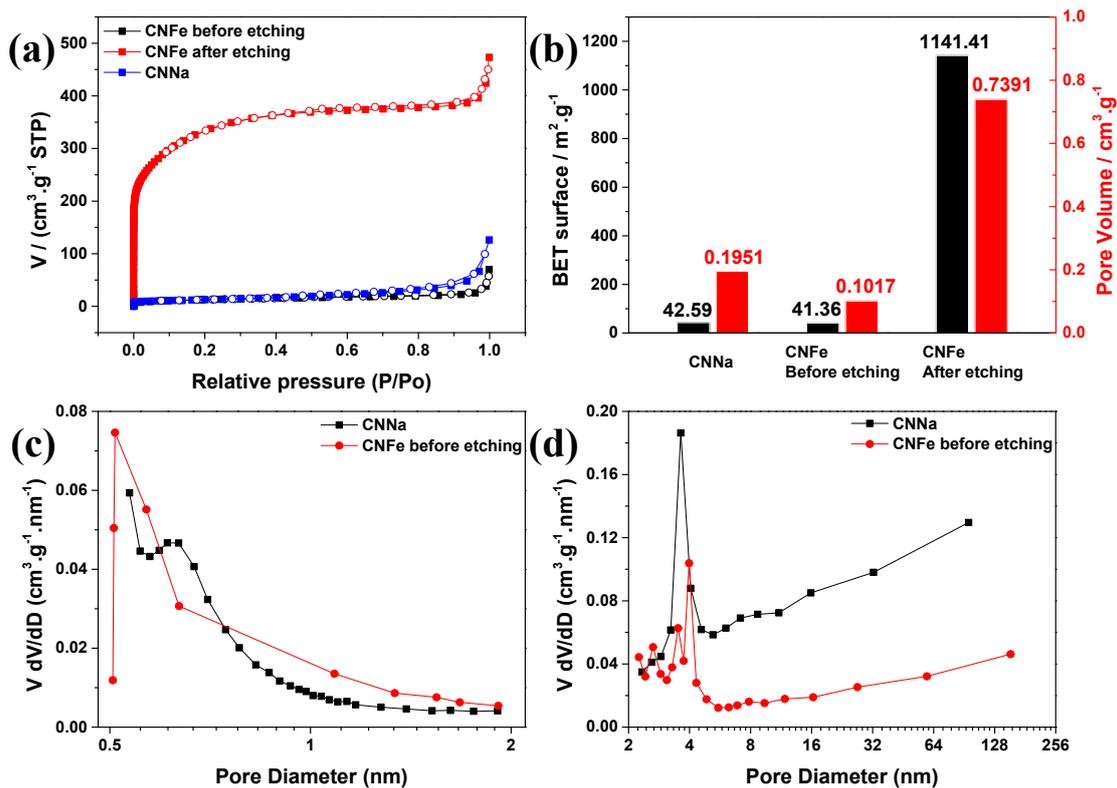
Fig. S3. (a) N_2 adsorption and desorption isotherms and (b) BET surface areas and pore sizes of CNNa and CNFe before and after etching, (c, d) Pore size distribution of CNNa and CNFe before etching.
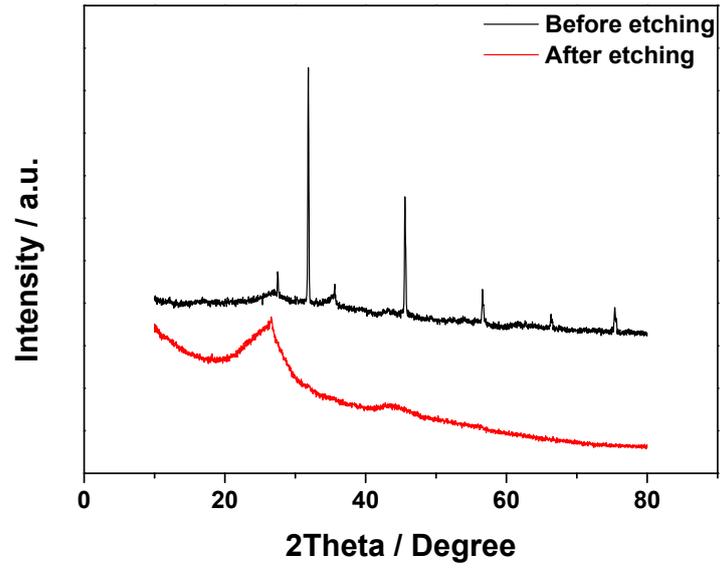
Fig. S4. XRD patterns of CNFe before and after etching.
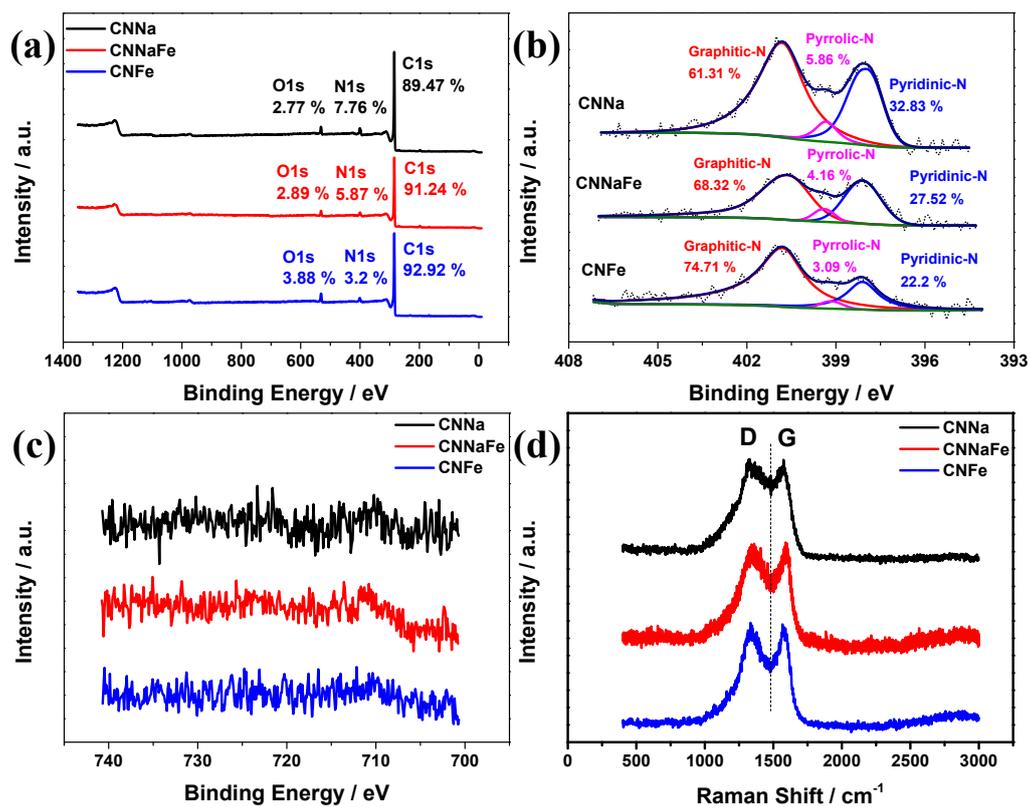
Fig. S5. (a) Full-scale XPS spectra of the catalysts, and high resolution of (b) N 1s and (c) Fe 2p. (d) Raman spectra of the CNNa, CNNaFe and CNFe.
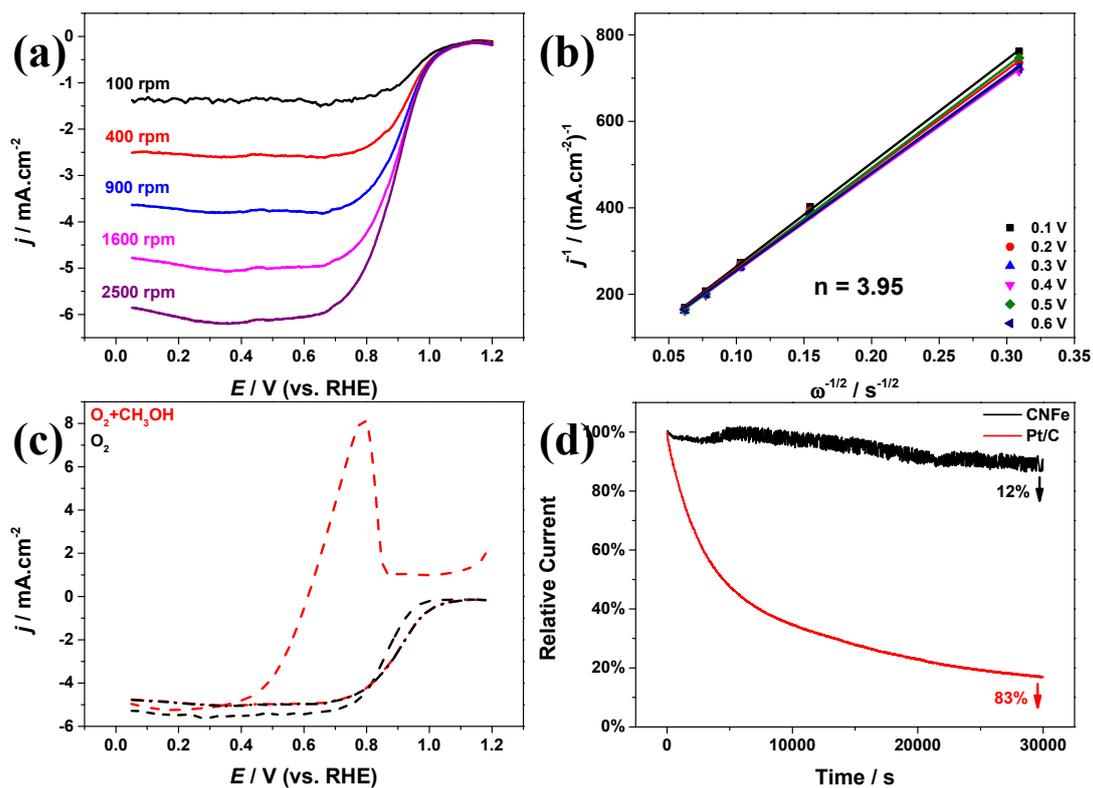
Fig. S6. (a) Voltamperograms for oxygen reduction on CNFe in O_2-saturated 0.1 M KOH at various rotation speeds; (b) Koutecky-Levich plots of CNFe at different potentials; (c) LSV of CNFe (dash dot line) and Pt/C (dash line) in O_2-saturated, 0.5 M methanol O_2-saturated and O_2-saturated 0.1 M KOH with a scan rate of 10 mV s^{-1}. (d) Current-time chronoamperometric responses of CNFe and Pt/C at 0.88 V (vs.RHE) in 0.1 M KOH at a rotation rate of 1600 rpm.
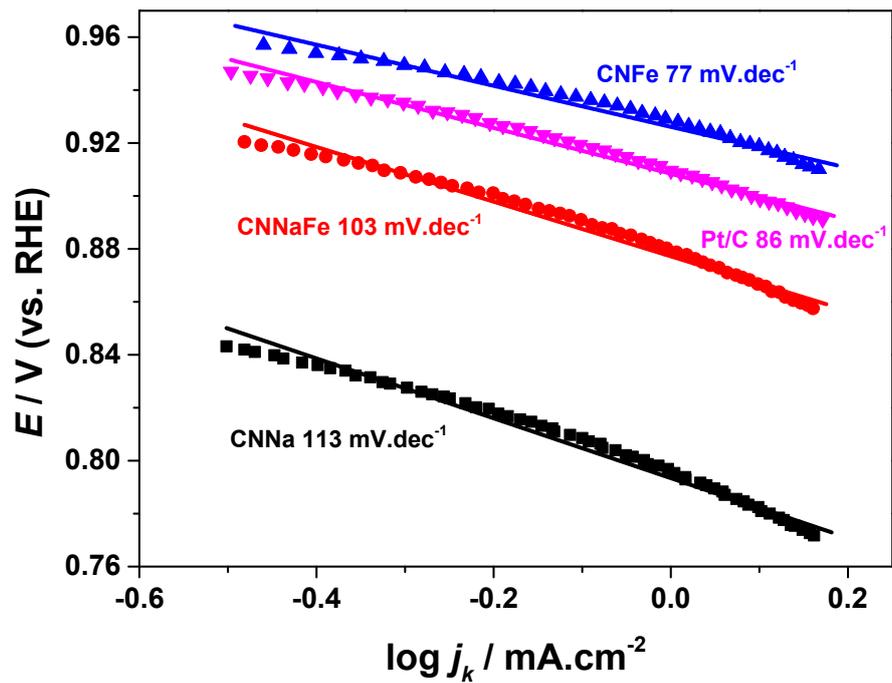
Fig. S7. The Tafel plot comparison of HPCMs with Pt/C.
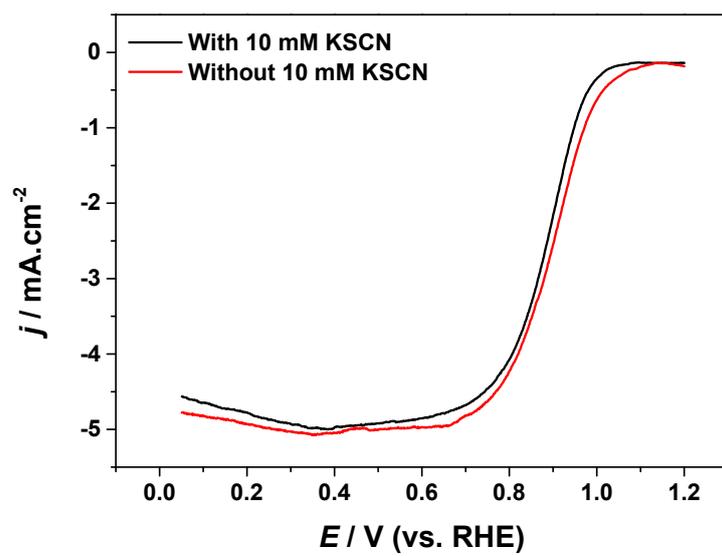
Fig. S8. Steady-state ORR polarization curves of CNFe catalyst in O_2-saturated 0.1 M KOH with or without 10 mM KSCN.
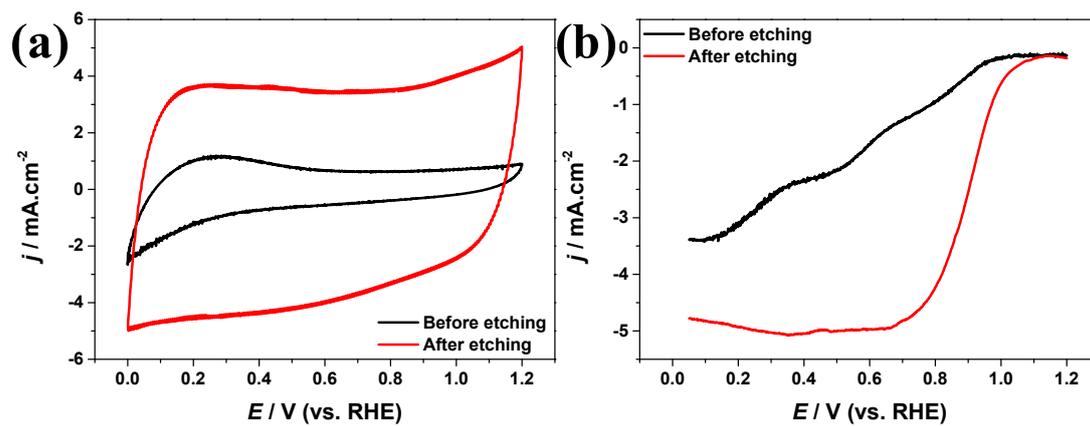
Fig. S9. CV and LSV curves of CNFe before and after etching in N_2 and O_2-saturated 0.1M KOH.
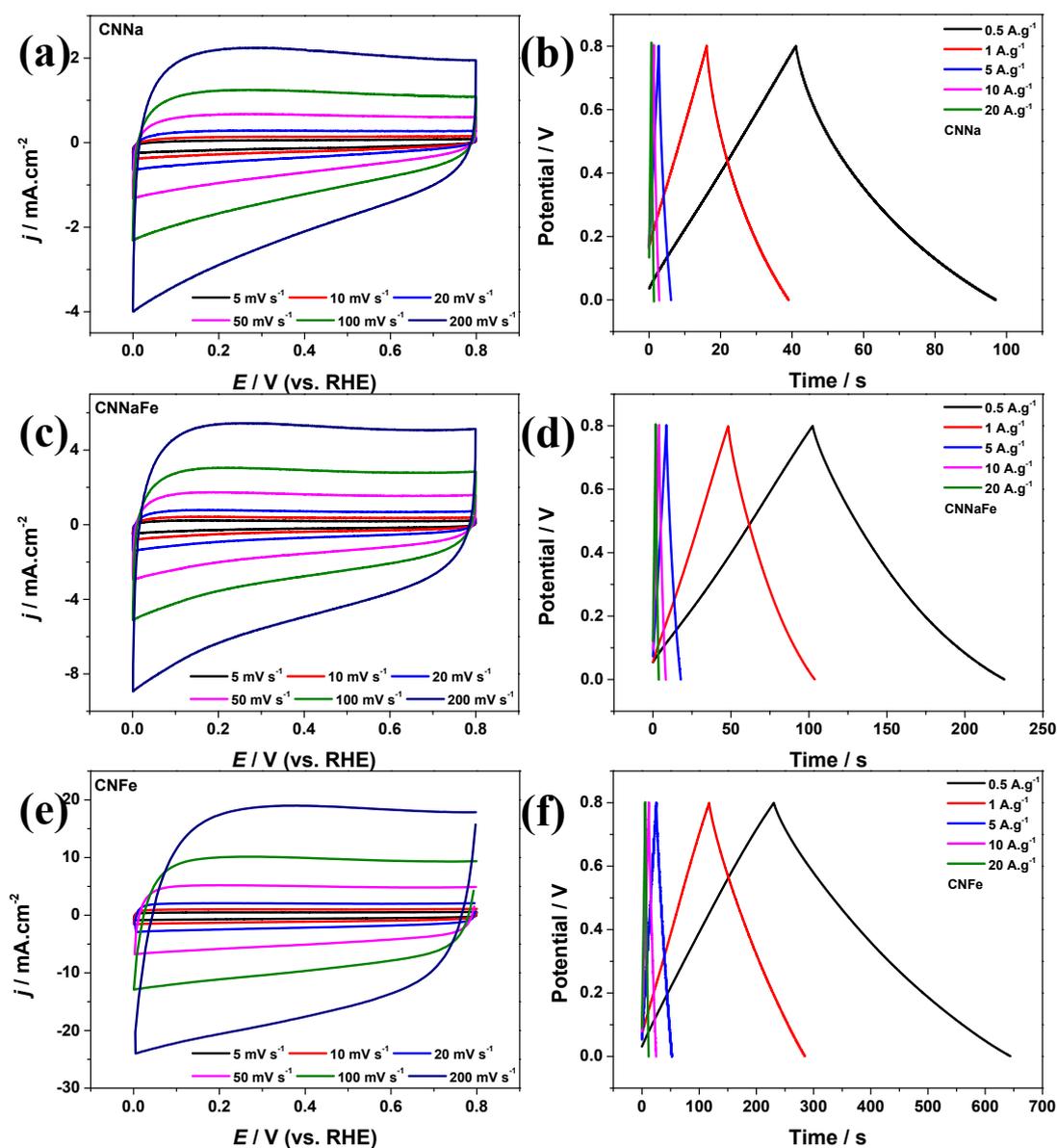
Fig. S10. CV and galvanostatic charge-discharge curves of (a, b) CNNa, (c, d) CNNaFe and (e, f) CNFe measured in a three-electrode system using 6 mol L^{-1} KOH as the electrolyte.

Table. S1. ORR performance of CNFe and some recently reported carbon-based materials. All electrocatalysts were tested in alkaline media.

Materials	Catalyst loading (mg cm^{-2})	Onset potential (V vs. RHE)	Half-wave potential (V vs. RHE)	Ref.
CNFe	**0.6**	**1.12**	**0.901**	**This work**
ISA Fe/CN	0.408	1.02	0.900	Angew. Chem. Int. ed., 2017, 129 (24): 7041-7045.
Fe@C-FeNC	0.7	1.01	0.899	J. Am. Chem. Soc., 2016, 138 (10): 3570-3578.
Fe-NMCSs	0.225	1.027	0.86	Adv. Mater., 2016, 28(36): 7948-7955.
O-NCNT-SS	0.6	1.052	0.885	Chem. Commun., 2017, 53(83): 11426-11429.
FeN2/NOMC		1.05	0.863	Nano Energy, 2017, 35: 9-16.
Fe©N-C-12	0.311	0.96	0.82	ACS Catal., 2017. 7 (11), 7638–7646
N-IOC-0.27-900	0.6	0.95	0.87	J. Mater. Chem. A, 2017, DOI: 10.1039/C7TA08354H
N,P-HPC	0.8	0.924	0.853	J. Mater. Chem. A, 2017, DOI: 10.1039/c7ta07746g

Table. S2. Supercapacitor of CNFe and some recently reported carbon-based materials. All electrocatalysts were tested in alkaline media.

Materials	Capacitance (F.g^{-1})	Rate	System	Ref.
CNFe	258	0.5 A/g	3	This work
Holey Graphene Oxide	283	1 A/g	3	Nano Lett. 2015, 15, 4605−4610
3D Graphene-like carbon	252	10mV/s	2	Carbon, 2017, 111 128-132
Ultrathin porous carbon shell	251	1 A/g	3	Carbon, 2017, 111 419-427
3D porous carbon fabrics	229	1 A/g	3	ACS Appl. Mater. Interfaces 2015, 7, 4257−4264
Graphene nanoribbons	189	0.1 A/g	2	Nature Chemistry, 2016, 8, 718-724
3D hierarchical carbon	188	1 A/g	3	Adv. Mater. 2016, 28, 5222–5228
Reduced graphene oxide	182	1 A/g	2	Chem. Commun., 2015, 51, 5598-5601.
NCM900	110	10 V/s	2	Nano Energy, 2016, 27: 482-491.